0026-895X/07/7106-1646–1656$20.00
MOLECULAR PHARMACOLOGY
Vol. 71, No. 6
30528/3210723
Mol Pharmacol 71:1646–1656, 2007
Printed in U.S.A.

Subunit-Stoichiometric Evidence for Kir6.2 Channel Gating, ATP Binding, and Binding-Gating Coupling[S]

Runping Wang, Xiaoli Zhang, Ningren Cui, Jianping Wu, Hailan Piao, Xueren Wang, Junda Su, and Chun Jiang

Department of Biology, Georgia State University, Atlanta, Georgia

Received September 5, 2006; accepted March 16, 2007

ABSTRACT

ATP-sensitive K^+ channels are gated by intracellular ATP, allowing them to couple intermediary metabolism to cellular excitability, whereas the gating mechanism remains unclear. To understand subunit stoichiometry for the ATP-dependent channel gating, we constructed tandem-multimeric Kir6.2 channels by selective disruption of the binding or gating mechanism in certain subunits. Stepwise disruptions of channel gating caused graded losses in ATP sensitivity and increases in basal P_{open}, with no effect on maximum ATP inhibition. Prevention of ATP binding lowered the ATP sensitivity and maximum inhibition without affecting basal P_{open}. The ATP-dependent gating required a minimum of two functional subunits. Two adjacent subunits are more favorable for ATP binding than two diagonal ones. Subunits showed negative cooperativity in ATP binding and positive cooperativity in channel gating. Joint disruptions of the binding and gating mechanisms in the same or alternate subunits of a concatemer revealed that both intra- and intersubunit couplings contributed to channel gating, although the binding-gating coupling preferred the intrasubunit to intersubunit configuration within the C terminus. No such preference was found between the C and N termini. These phenomena are well-described with the operational model used widely for ligand-receptor interactions.

ATP-sensitive K^+ channels (K_{ATP}) play an important role in insulin secretion, glucose uptake, myocardium excitability, and neuronal responses to metabolic stress (Ashcroft and Gribble, 1998; Seino, 1999). Such functions rely on the sensitivity of channels to intracellular ligand molecules. K_{ATP} channel activity is inhibited by intracellular ATP and activated by ADP, proton, and phospholipids (Noma, 1983; Baukrowitz et al., 1998; Shyng and Nichols, 1998; Xu et al., 2001). Like other ligand-gated ion channels, the interaction of ligands with K_{ATP} channels (ligand binding) is believed to trigger a cascade of conformational changes of individual subunits, leading to alternations in channel open or closed states. The latter step is known as channel gating. In addition, there are intermediate steps known as signal transduction or coupling. This scenario has been supported by a number of previous studies (Perozo et al., 1999; Flynn and Zagotta, 2001; Jiang et al., 2002; Jin et al., 2002; Phillips et al., 2003).

Because most of the previous studies were done on homomeric channels of wt or mutants, it is unclear how individual subunits in a multimeric channel act in ligand binding, channel gating, and their couplings and how they are coordinated in the ligand-dependent gating. To address these questions, we performed studies on tandem-dimeric and tandem-tetrameric channels constructed with a predetermined number of subunits disrupted with T71Y, C166S, and K185E mutations. The Lys185 plays a role in ATP binding (Trapp et al., 2003; Antcliff et al., 2005; John et al., 2005) but is not involved in sensing sulfonylurea, protons, and lipid metabolites (Wu et al., 2002; Ribalet et al., 2003). Mutation of Lys185 to a negatively charged residue causes almost complete loss of ATP sensitivity, whereas its mutation to a nonpolar residue has rather mild effects on the ATP sensitivity (Reimann et al., 1999). In contrast, the Cys166 located in the transmembrane 2 region (Supplemental Fig. S1) is known to participate in the channel gating or the final stage of signal transduction, because the C166S mutation disrupts K_{ATP} channel gating by ATP, proton, and sulfonylurea (Trapp et al., 1998; Piao et al., 2001; Wu et al., 2004). Likewise, the Thr71 at the intracellular end of the transmembrane 1 region is likely to act in channel gating by ATP and protons as well (Cui et al., 2003; Wang et al., 2005b). Studies on the subunit stoichiometry of the K_{ATP} channels, whose ATP binding or channel gating is disrupted with these residues, thus may yield information about the subunit coordination, cooperativity, and minimal requirement of functional subunits for the ATP-

This work was supported by National Institutes of Health grant HL67890.
Article, publication date, and citation information can be found at http://molpharm.aspetjournals.org.
doi:10.1124/mol.106.030528.
[S] The online version of this article (available at http://molpharm.aspetjournals.org) contains supplemental material.

ABBREVIATIONS: K_{ATP}, ATP-sensitive K^+ channels; wt, wild type; *h*, Hill coefficient; HH, Hodgkin-Huxley; MWC, Monod-Wyman-Changeux.

dependent gating. They may also shed insight into subunit contributions to ligand binding, channel gating, and potential coupling mechanism of ligand binding to channel gating.

Materials and Methods

Mouse Kir6.2 (mBIR, GenBank accession number D50581) cDNAs were generously provided by Dr. S. Seino (Kobe University, Kobe, Japan). The cDNAs were subcloned to a eukaryotic expression vector (pcDNA3.1; Invitrogen, Carlsbad, CA). To construct the tandem-dimeric and tandem-tetrameric channels, a cassette was generated with a BamHI restriction site introduced at the 5′-end and a BglII site introduced at the 3′-end of the Kir6.2ΔC36 open reading frame using polymerase chain reaction. Based on the cassette, site-specific mutation of Lys185 to glutamic acid and the stop codon to serine were then prepared (Cui et al., 2003; Wu et al., 2004; Wang et al., 2005b). The cDNA of wild-type Kir6.2ΔC36 without stop codon was linearized with restriction enzyme BglII. The mutant cDNA of K185E with stop codon was digested with restriction enzymes BamHI and BglII. The isolated mutant K185E fragment was then ligated to the linearized wt Kir6.2ΔC36 to form the dimeric wt-K185E. There are three amino acids (serine-arginine-serine) created between each monomer as linker. The tandem dimers wt-wt and K185E-K185E were constructed using the same strategy.

The cohesive end of BamHI site and BglII site is complimentary, which allows mutual DNA ligation. Because both restriction sites are lost after ligation, the dimer still contains only one BamHI site upstream of the start codon and a BglII site downstream of the stop codon. This allows construction of the tandem-tetrameric channel using the same strategy. To do so, a second set of dimers was constructed with the stop codon eliminated, which was joined with another dimer with stop codon. Various tetrameric concatemers were constructed using the combination of two sets of dimers. The correct orientation of the constructs was confirmed by identifying appropriate peaks in DNA sequence and correct size with two restriction enzymes. Other tandem-dimeric tandem-tetrameric channels with mutation of T71Y and C166S were similarly constructed. To prove the lack of random subunit assembly, we constructed one dimeric and two tetrameric channels, with one subunit carrying G132S mutation. This dominant-negative mutation is known to produce nonfunctional channels.

Frog oocytes were obtained from *Xenopus laevis* as described previously (Xu et al., 2001; Cui et al., 2003; Wu et al., 2004; Wang et al., 2005a). Two-electrode voltage clamps were used to screen the expression 3 to 4 days after cDNA injection. Whole-cell currents were recorded using an amplifier (Geneclamp 500; Axon Instruments Inc., Foster City, CA) at ~24°C. The extracellular solution contained 90 mM KCl, 3 mM $MgCl_2$, and 5 mM HEPES, pH 7.4.

Patch clamp was performed using a bath solution containing 10 mM KCl, 105 mM potassium gluconate, 5 mM KF, 5 mM potassium pyrophosphate, 0.1 mM sodium vanadate, 5 mM EGTA, 5 mM glucose, and 10 mM HEPES, pH 7.4. The pipette was filled with the same solution (Wang et al., 2005a). Pyrophosphate and vanadate are known to alleviate channel rundown. With the solution, there was only modest or no channel rundown in 10 min when most of recordings were done (Figs. 1 and 3). Single-channel conductance was measured using ramp command potentials from 100 to −100 mV. The open-state probability (P_{open}) was calculated by first measuring the time, t_j, spent at current levels corresponding to $j = 0, 1, 2, \ldots n$ channels open, based on all evident openings during the entire period of record. The P_{open} was then obtained as

$$P_{open} = \frac{\sum_{j=1}^{n} t_j \cdot j}{T \cdot n} \quad (1)$$

where n is the number of channels active in the patch, and T is the duration of recordings. P_{open} values were calculated from at least four stretches of data acquired using the Clampfit 9.2 software (Axon Instruments).

The operational model was used to described our data based on the transduction mechanism (Scheme 1) proposed by Del Castillo and Katz (1957). A ligand A binds to a vacant receptor R to form the complex AR, depending on their binding affinity K_A. A fraction of the AR complex is then active (AR*), which is controlled by the equilibrium constant τ. The ATP-P_{open} relationship of the K185E-concatenated tetramers was fitted with the modified equation of the operational model (Black and Leff, 1983):

$$P_{open} = P_{OB} - \frac{[ATP]^h \cdot \tau_A{}^h}{(K_A + [ATP])^h + \tau^h \cdot [ATP]^h} \quad (2)$$

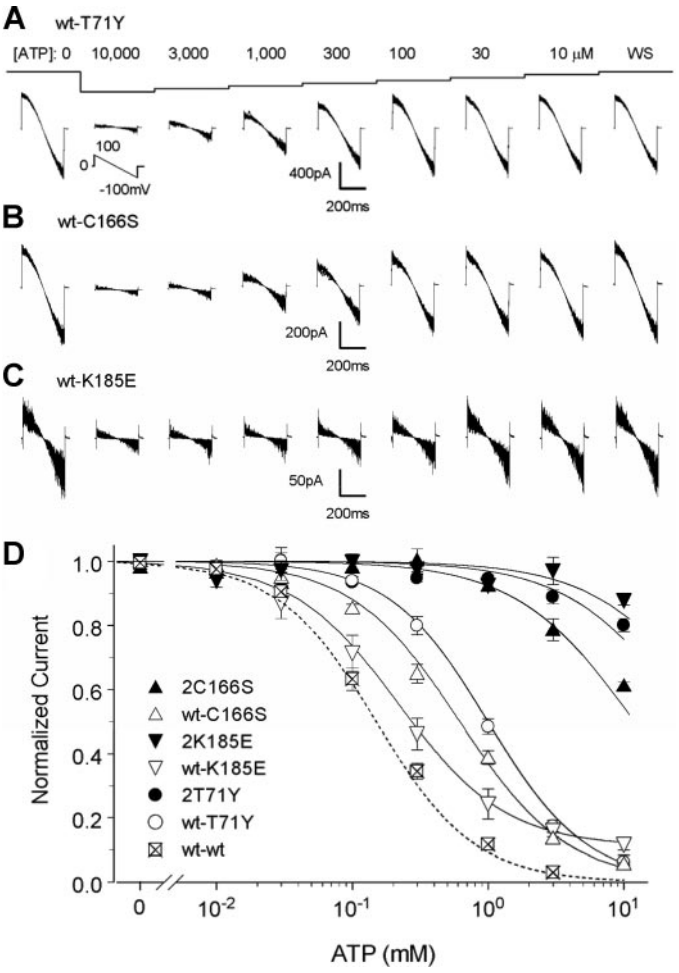

Fig. 1. ATP response of the tandem-dimeric Kir6.2 channels. Intracellular ATP produced dose-dependent inhibition in the heteromeric wt-T71Y (A) and wt-C166S (B) dimers. The currents were almost completely inhibited by 10 mM ATP. C, although the wt-K185E currents were also inhibited, the inhibitory effect reached the plateau with 1 mM ATP, and there were still substantial currents uninhibited. D, the dose-response curves of the homomeric wt and mutant dimers show the same ATP sensitivity to their monomeric counterparts. The curves of the heteromeric wt-C166S and wt-T71Y dimers lay in between the wt-wt and mutant dimers with the curves closer to the wt-wt channel. The ATP-current relationship for the wt-K185E dimer was special, because the maximum inhibition is ~90% at the plateau level with 10 mM ATP.

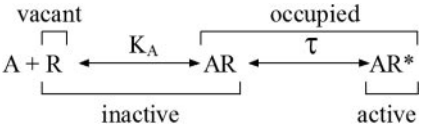

Scheme 1. Schematic for receptor-ligand interaction.

where P_{OB} is the basal P_{open} without ligand, h is Hill coefficient, τ_A is operational efficacy obtained from eq. 3, and K_A is the equilibrium dissociation constant for ligand binding obtained from eq. 4. According to Scheme 1, the K_A indicates binding affinity of the ligand-receptor complex, and τ_A is a measure of transduction efficiency of occupied receptors or the magnitude of the first step of conformational change after ligand binding (Black and Leff, 1983; Trzeciakowski, 1999a,b).

$$P_{AR^*} = \frac{\tau_A{}^h}{\tau_A{}^h + 1} \quad (3)$$

where P_{AR^*} equals to the difference of P_{OB} and steady-state levels of P_{open} in the presence of ligands (P_{OT}) (i.e., $P_{AR^*} = P_{OB} - P_{OT}$), indicating the maximum fraction of receptors in the active state. The P_{AR^*} is 50% of maximum when $\tau_A = 1$ and $h = 1$, and it is 90% or higher when $\tau_A > 10$. The maximum ligand effect (E_{max}) is calculated as $E_{max} = P_{AR^*}/P_{OB}$. The IC_{50} is a function of K_A and τ_A.

$$IC_{50} = \frac{K_A}{(2 + \tau_A{}^h)^{1/h} - 1} \quad (4)$$

Accordingly, τ_A has an effect on IC_{50} and E_{max}. A similar equation was used to describe the C166S- and T71Y-concatenated tetramers:

$$P_{open} = P_{OB} - \frac{[ATP]^h \cdot \tau_C{}^h}{(K_C + [ATP])^h + \tau_C{}^h \cdot [ATP]^h} \quad (5)$$

where K_C is the affinity constant determined by K_A and τ_A (see *Discussion* for their relationship), and τ_C is efficacy controlling the range of the second step of conformational change for gating/coupling. The K_C and τ_C were calculated similarly as K_A and τ_A using eqs. 3 and 4.

Data are presented as means ± S.E.. All patch data reported were based on four or more patches obtained from at least two oocytes. Differences of ATP effects with ATP exposures were examined using analysis of variance or Student's t tests and were considered statistically significant if $P \leq 0.05$.

Results

Selective Suppression of ATP-dependent Channel Gating. The Kir6.2ΔC36 channel was expressed in *X. laevis* oocytes. The rationale for choosing this form of K_{ATP} channels was 1) the truncation of 36 residues at the C terminus allows the Kir6.2 to be expressed without the SUR subunit with much of the ATP sensitivity retained (Tucker et al., 1997); and 2) it can simplify the studies of ATP-dependent channel gating by dissecting the contribution from the SUR subunit. Expression of the channel was screened by two-electrode voltage clamp using a bath solution (KD90) containing 90 mM K^+. Cells showing clear inward-rectifying K^+ currents were used for further patch-clamp studies. Injection of the expression vector alone did not yield inward-rectifying currents. Exposure of intracellular membranes to perfusates with various ATP levels produced a concentration-dependent inhibition of the currents. The ATP-current relationship was described with the Hill equation. The ATP concentration for 50% current inhibition (IC_{50}) was 110 μM ($n = 12$) and the Hill coefficient (h) was 1.2 ($n = 12$) (Supplemental Fig. S2, A and E). The ATP sensitivity was mostly eliminated with either C166S, K185E, or T71Y mutation, (Supplemental Fig. S2, B–D, and Table 1).

The Kir6.2ΔC36 channel is also gated by intracellular protons, in which a protonation site (His175) has been identified previously (Xu et al., 2001). The pH-dependent channel gating was lost with the T71Y or C166S mutation, suggesting a role of these residues in channel gating (Supplemental Fig. S2, E and F). In contrast, the K185E mutation disrupted the ATP-dependent but not the pH-dependent channel gating (Supplemental Fig. S2, E and F), supporting that the Lys185 contributes to ATP binding as reported in several previous studies (Reimann et al., 1999; Ribalet et al., 2003; Trapp et al., 2003; Antcliff et al., 2005; John et al., 2005).

In control experiments, we tested two tandem-tetrameric channels that carried the G132S dominant-negative mutation in the first and last subunit, respectively. Expression of these constructs was attempted in *X. laevis* oocytes. Each construct was injected in >60 oocytes followed by whole-cell voltage clamp. The same experiments were then repeated in >60 oocytes for every constructs. The repetitive tests in a large number of cells ($n > 120$ for each construct) failed to show any detectable inward-rectifier currents. In addition, we tested a tandem-dimer with the G132S mutation in the first subunit. It did not express functional currents either. In contrast to these G132S constructs, all Kir6.2 dimers and tetramers used in the present study showed clear whole-cell inward-rectifier currents, indicating that these Kir6.2 tandem-multimers do not form a tetrameric channel by a random subunit assembly.

Effects of Heteromeric Recombination of Tandem-Dimeric Channels. To understand the subunit stoichiometry of Kir6.2 channel gating by intracellular ATP, we first constructed tandem-dimeric channels by linking the wt Kir6.2ΔC36 and C166S-mutant subunits in wt-wt, wt-C166S, and C166S-C166S configurations. All of these dimers expressed functional currents without significant changes in inward rectification, current amplitude, and other single-channel properties in comparison with their monomeric counterparts. Currents of the wt-wt channel were dose-dependently inhibited by ATP with IC_{50} 150 μM ($n = 7$) and h value 1.2 ($n = 7$). Complete current inhibition was reached with 3 mM ATP (Fig. 1D and Table 1). The ATP sensitivity was eliminated in the C166S-C166S dimer with IC_{50} value of 9 mM, consistent with the monomeric C166S. The ATP sensitivity of the heteromeric wt-C166S dimer lay in between the homomeric wt-wt and C166S-C166S channels. The wt-C166S showed an IC_{50} value of 0.62 mM and an h value of 1.0 (Fig. 1, B and D, and Table 1). The C166S-wt dimer showed similar ATP sensitivity.

Similar constructions were also done for the Thr71. The ATP sensitivity of the T71Y-T71Y dimer was comparable with the monomeric T71Y channel (Fig. 1D). Like the C166S dimers, the ATP sensitivity of the wt-T71Y was closer to the wt-wt channel than the T71Y-T71Y dimer, in which a parallel shift of the ATP-current relationship curve was observed. The IC_{50} value increased to 1.0 mM with an h value 1.2 (Fig. 1, A and D, and Table 1).

The homomeric K185E-K185E responded to the intracellular ATP like the K185E monomer, whereas the wt-K185E currents were not totally inhibited even with high concentrations of ATP (Fig. 1, C and D). In contrast to the wt-T71Y and wt-C166S channels, there were still ~9.7% residual currents left uninhibited under 30 mM ATP in the wt-K185E (Table 1), although its IC_{50} value was only 70 μM higher than that of the wt-wt channel (Fig. 1D and Table 1), suggesting that subunit stoichiometry for ligand binding is different from that for channel gating.

Subunit Stoichiometry for ATP Binding. To further understand the subunit stoichiometry of the ATP binding, tetrameric concatemers were constructed with the wt and K185E-disrupted subunits. The channels with two functional subunits located at adjacent and diagonal positions were named *cis* and *trans* 2wt-2K185E. Similar to the dimeric wt-K185E, the open-state probability (P_{open}) of several K185E-concatenated tetramers were not fully inhibited with 30 mM ATP (Figs. 2 and 3), although their IC_{50} levels were rather low. Such an effect was not limited to Kir6.2ΔC36, because the uninhibited residual currents were also observed in K185E-Kir6.2/SUR1 (Supplemental Fig. S3). In the presence of substantial uninhibited channel activity, the ATP-current relationship of these K185E-concatenated tetramers can no longer be described using the conventional Hill equation without counting the levels of maximum inhibition. Indeed, the ATP-current relationship resembles partial antagonism for ligand-receptor interaction (Kenakin, 2004), suggesting that the subunit disruption causes a loss of not only potency but also efficacy and maximum ligand effect (E_{max}).

The changes in potency, efficacy, and E_{max} have been described successfully with the operational model for ligand-receptor interactions (Black and Leff, 1983; Kenakin, 2004). This model, however, has not been applied to the ion channel studies, although it is highly recommended (Colquhoun, 1998). The model describes multiple steps of events of the ligand-receptor interaction (i.e., formation of ligand-receptor complex, the consequent conformational change with the ligand binding, and signal transduction) (Black and Leff, 1983; Colquhoun, 1998; Trzeciakowski, 1999a; Kenakin, 2004). Therefore, we used the operational model to describe the subunit stoichiometry of the K185E-concatenated tetramers (see *Materials and Methods*). The operational model takes account of five events: K_A, efficacy (τ_A), potency (IC_{50}), basal P_{open}, and maximum channel inhibition by ATP (E_{max}). The latter three can be obtained from experiments.

Because there is no significant difference in the basal P_{open} of all K185E constructs (Table 1), an average of basal P_{open} (0.116) was used for the data fitting. The construct with all four subunits disrupted showed very low ATP sensitivity ($K_A > 20$ mM, $\tau_A < 0.05$, and $IC_{50} > 20$ mM) (Fig. 4A). When the first wt subunit was introduced, the wt-3K185E channel gained ATP sensitivity drastically ($IC_{50} = 530$ μM, $h = 0.9$). The increase in ATP sensitivity was caused by a great increase in the ATP binding affinity ($K_A = 650$ μM), although

TABLE 1

Measurements and predictions of Kir6.2 constructs

All mutant channels were constructed on Kir6.2ΔC36. Residue currents (I) were measured as a portion of maximal channel activity in the presence of 30 mM ATP. Data are presented as means ± S.E.

Construct	P_{OB}	E_{max}	Hill equation		n	Operational Model		
			IC_{50}	h		τ_A/τ_C	K_A/K_C	IC_{50}
		%	*mM*				*mM*	*mM*
Monomer								
Kir6.2ΔC36	N.A.	100.0	0.11	1.2	12	N.A.	N.A.	N.A.
K185E	N.A.	N.A.	>20	1.2	4	N.A.	N.A.	N.A.
C166S	N.A.	N.A.	8.00	N.A.	4	N.A.	N.A.	N.A.
T71Y	N.A.	N.A.	>20	N.A.	4	N.A.	N.A.	N.A.
Tandem-dimer								
wt-wt	N.A.	100.0	0.15	1.1	7	N.A.	N.A.	N.A.
wt-K185E	N.A.	90.3	0.22	1.1	5	N.A.	N.A.	N.A.
K185E-K185E	N.A.	N.A.	>20		4	N.A.	N.A.	N.A.
wt-C166S	N.A.	100.0	0.62	1.0	4	N.A.	N.A.	N.A.
C166S-C166S	N.A.	N.A.	9.00	1.0	5	N.A.	N.A.	N.A.
wt-T71Y	N.A.	100.0	1.00	1.2	4	N.A.	N.A.	N.A.
T71Y-T71Y	N.A.	N.A.	>20	1.1	5	N.A.	N.A.	N.A.
Tandem-tetramer								
4wt	0.116	100.0	0.15	1.2	10	0.19	0.13	0.15
K185E								
3wt-K185E	0.118	100.0	0.17	1.1	4	0.16	0.18	0.18
cis 2wt-2K185E	0.127	95.6	0.18	1.1	4	0.15	0.18	0.18
trans 2wt-2K185E	0.116	87.3	0.23	1.1	6	0.14	0.23	0.24
wt-3K185E	0.120	80.3	0.60	0.9	7	0.08	0.65	0.53
4K185E	0.120	N.A.	>20	0.9	5	0.03	>20	>20
C166S								
3wt-C166S	0.180	100.0	0.17	1.2	5	0.28	0.18	0.19
cis 2wt-2C166S	0.514	99.2	0.72	1.2	4	1.05	1.15	0.75
trans 2wt-2C166S	0.497	99.2	0.72	1.2	5	1.05	1.15	0.75
wt-3C166S	0.556	N.A.	1.80	1.1	4	1.29	3.60	1.82
4C166S	0.723	N.A.	7.00	1.1	4	2.50	>20	6.74
T71Y								
3wt-T71Y	0.490	100.0	0.25	1.1	4	1.00	0.38	0.22
cis 2wt-2T71Y	0.540	99.2	1.10	1.2	4	1.10	1.80	1.14
trans 2wt-2T71Y	0.511	99.2	1.10	1.2	4	1.10	1.80	1.14
wt-3T71Y	0.736	N.A.	6.00	1.1	4	2.50	18.00	5.78
4T71Y	0.738	N.A.	>20	1.1	4	2.50	>20	>20
Coupling dimer								
wt-K185E/C166S	0.538	72.2	0.78	1.0	5	0.65	1.40	0.85
K185E-C166S	0.542	49.4	1.10	1.0	5	0.42	1.70	1.20
wt-K185E/T71Y	0.545	53.4	1.10	1.0	4	0.42	1.70	1.20
K185E-T71Y	0.581	48.2	1.10	1.0	4	0.42	1.70	1.20

h, Hill coefficient; n, number of observation; N.A., not available.

the efficacy (τ_A = 0.08) and E_{max} (80.3%) were still low (Figs. 3A and 4A). Another significant gain in ATP sensitivity was seen with the addition of the second wt subunit at the *trans* position (IC_{50} = 240 μM, h = 1.1), which was contributed by both K_A (230 μM) and τ_A (0.14). The E_{max} value was improved to 87.3%. The ATP binding affinity (K_A = 180 μM), efficacy (τ_A = 0.15), and E_{max} (95.6%) were further increased in the *cis* 2wt-2K185E with a reduction in IC_{50} (180 μM), suggesting that ATP prefers two subunits at adjacent positions. It is interesting that introduction of the third wt subunit produced almost no change in the ATP sensitivity (IC_{50} = 180 μM, h = 1.1) with nearly the same K_A (180 μM) and τ_A (0.16) levels as the *cis* 2wt-2K185E, although the E_{max} reached 100%. The IC_{50} value was lowered to 150 μM with the fourth wt subunit because of the improved K_A (130 μM) and τ_A (0.19) values.

For a comparison purpose, we also fitted the data with the Hill equation. The IC_{50} and h values obtained were compa-

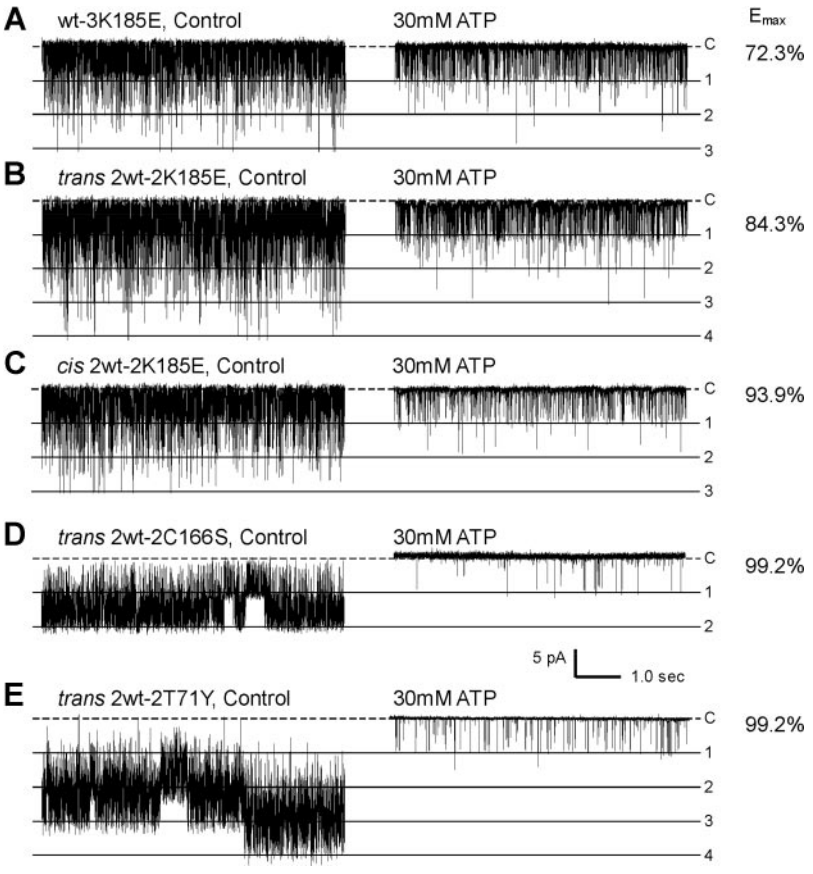

Fig. 2. Single-channel activity of tetrameric channels recorded with and without ATP. Although all channels were inhibited by 30 mM ATP, substantial uninhibited currents were seen in constructs containing K185E mutations. The maximum inhibition was calculated based on the P_{open} value with ATP (P_{OT}) and that without (P_{OB}). $E_{max} = (1 - P_{OT}/P_{OB}) \times 100\%$, which was 72.3% for the 3wt-K185E (A), 84.7% for the *trans* 2wt-2K185E channel (B), and 93.9% for the *cis* 2wt-2K185E channel (C). In contrast, the *trans* 2wt-2C166S (D) and *trans* 2wt-2T71Y channels (E) were almost completely inhibited by 30 mM ATP with maximum inhibition more than 99%.

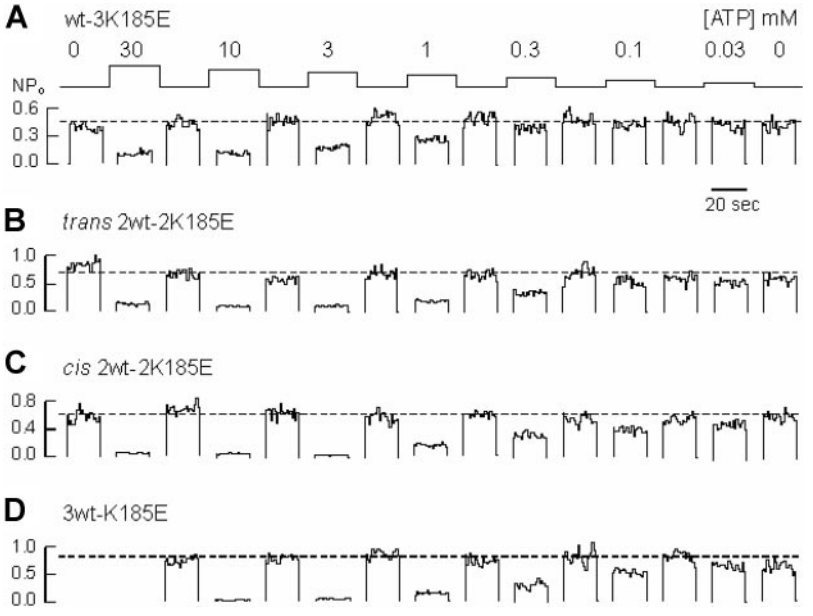

Fig. 3. Effects of intracellular ATP on the channel activity of tetrameric K185E constructs. A, single-channel activity was recorded with the membrane potential held at −80 mV. The P_{open} value was obtained with each ATP concentration. Fast and reversible inhibition in the single-channel activity was seen in the wt-3K185E. The inhibition reached the maximum level with 10 mM ATP, and no further inhibition was found with higher concentrations. B, the inhibitory effect of ATP was stronger in the *trans* 2wt-2K185E, and the maximum inhibition was reached with 10 mM. C, the ATP sensitivity further increased in the *cis* 2wt-2K185E, and 3 mM ATP produced maximum effect. Note that the residue channel activity reduces with increasing numbers of wt subunits. D, the 3wt-K185E was fully inhibited with 10 mM ATP.

rable with those predicted with the operational model (Fig. 4, A and B, and Table 1).

Subunit Stoichiometry for Channel Gating. To understand the subunit stoichiometry for channel gating, tandem-tetrameric channels were constructed with C166S-disrupted subunits whose ATP sensitivity was comparable with the corresponding monomeric and dimeric channels (Fig. $5A_2$ and Table 1). A prominent effect of the C166S-subunit disruptions was a graded increase in baseline channel activity. The basal P_{open} value increased from 0.116 in the wt channel to 0.723 in the 4C166S, whereas other constructs showed intermediate levels of baseline P_{open} (Table 1). Previous mutational analysis of homomeric channels has shown that the Cys166 mutation disrupts the long closures (Trapp et al., 1998). Consistent with these previous observations, our results showed that the ATP sensitivity decreased gradually with introducing more C166S subunits (Fig. $5A_2$). Because both the ATP sensitivity and the magnitude of channel activity changed in the C166S constructs, we also used the operational model to describe the ATP-current relationship. Based on the basal P_{open}, E_{max}, and IC_{50} values, the K_C and τ_C values were calculated according to eqs. 3 and 4 under *Materials and Methods*. Our results showed that the τ_C value increased from 0.19 to 2.50, and K_C changed from 0.15 to 21.00 mM with stepwise C166S-subunit disruptions. These led to a change in IC_{50} levels similar to those described with the Hill equation (Fig. 5, A_1 and A_2). It is remarkable that the disruption of channel gating did not change the E_{max} value but increased the basal P_{open} value significantly, in clear contrast to ATP binding disruptions.

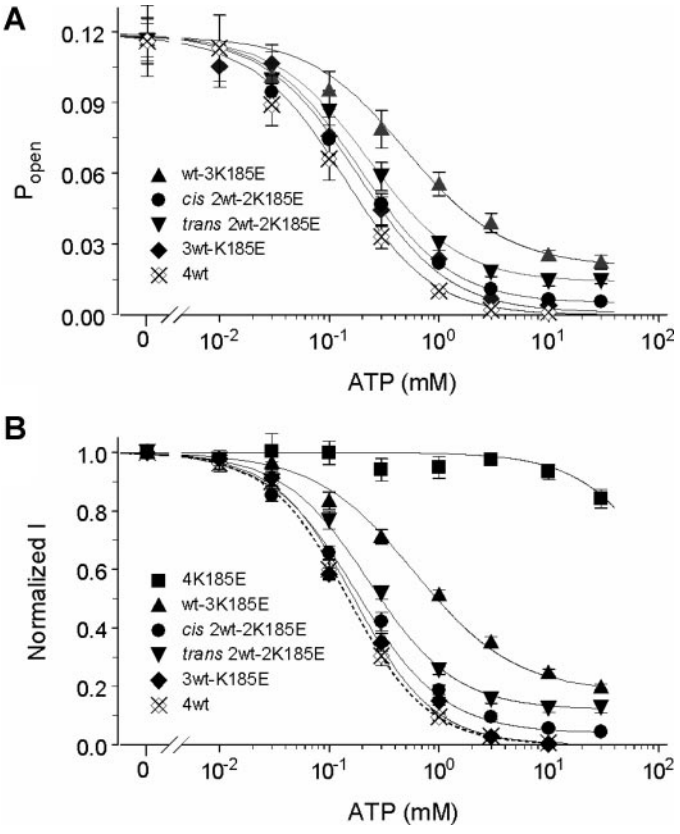

Fig. 4. Description of ATP sensitivity of tetrameric K185E constructs with two different models. A, the single-channel activity is expressed as a function of the intracellular ATP concentration using eq. 2 based on the operational model (see *Materials and Methods*). The basal P_{open} value averages 0.116. The ATP sensitivity and the maximum inhibitory effect increase with more wt subunits. ATP has larger inhibitory effect on the *cis* 2wt-2K185E than on the *trans* 2wt-2K185E. Incomplete inhibition is seen in channels carrying more than two disrupted subunits. B, the ATP-current relationship curves are also fitted with Hill equation after normalizing the baseline activity to 1.0. The IC_{50} levels obtained are comparable with those calculated with operational model (Table 1).

A similar trend was also seen in tetramers carrying T71Y mutation. With the addition of T71Y-disrupted subunits, the basal P_{open} increased from 0.116 to 0.738, K_A changed from 0.13 to >20 mM, and the τ_C increased from 0.19 to 2.50. The predicted IC_{50} values (0.15 to >20 mM) were also similar to those measured with the Hill equation in these mutations (Fig. 5, B_1 and B_2, and Table 1). Also similar to the C166S constructs was the unchanged E_{max} value with graded subunit disruptions. The IC_{50} and h values of *trans* 2wt-2T71Y were almost identical with those of *cis* 2wt-2T71Y and wt-T71Y dimers.

Subunit Cooperativity and Coordination. To elucidate the subunit cooperativity and coordination, we plotted the IC_{50} values against the number of wt subunits and compared our results to two classes of models with and without cooperativity. The Hodgkin-Huxley (HH) model describes channel-gating process produced by independent action of individual subunits (Hodgkin and Huxley, 1952), whereas the Monod-Wyman-Changeux (MWC) model describes positive cooperativity, in which four subunits undergo a single concerted transition between channel opening and closure (Monod et al., 1965; see Supplemental Methods for details about the prediction using these two models). We found that our data could not be described with the HH model (Fig. 6, A–C), suggesting that four subunits do not act independently in either ATP binding or channel gating. The IC_{50} plot of K185E constructs was far from the MWC prediction and even went lower than the HH prediction (Fig. 6A), suggesting the existence of negative cooperativity between subunits in ATP binding. In contrast, the IC_{50} plots of the C166S and T71Y tetramers were located in between those predicted by the MWC and HH models (Fig. 6, B and C), suggesting moderate positive cooperativity. Further supporting the presence of positive cooperativity in channel gating were the basal P_{open} plots against the number of wt subunits, because the basal P_{open} plots were superimposed or even greater than the values predicted by the MWC model (Fig. 6, E and F).

These plots also suggested special forms of subunit coordination for ligand binding and channel gating (Fig. 6, E and F). Interruption of the ATP binding did not alter the baseline P_{open} of the K185E-disrupted channels (Fig. 6D). Changes in baseline P_{open} were only seen when the binding-gating coupling was disrupted with C166S or T71Y mutations. In tetramers with the C166S mutation, the basal P_{open} value was greatly reduced by introducing the first wt subunits, whereas the second one gave rise to a smaller effect. The pattern of baseline P_{open} changes was nicely repeated when the third and fourth subunits were introduced (Fig. 6E), indicating the existence of functional dimers between subunits, as shown previously in other ion channels (Liu et al., 1998). Such a subunit coordination was also found in the T71Y tetramers. The pattern of baseline P_{open} changes repeated when every other wt subunit was introduced, although the major contribution came from the introduction of the second and fourth wt subunits (Fig. 6F).

Intersubunit Coupling. To gain insight into the coupling mechanisms of ATP binding to channel gating in the Kir6.2 channel, concatenated dimers were constructed with the disruption of ATP binding or gating in the same or alternate subunit. We reasoned that if the coupling only existed within the same subunit (i.e., intrasubunit coupling), it would be

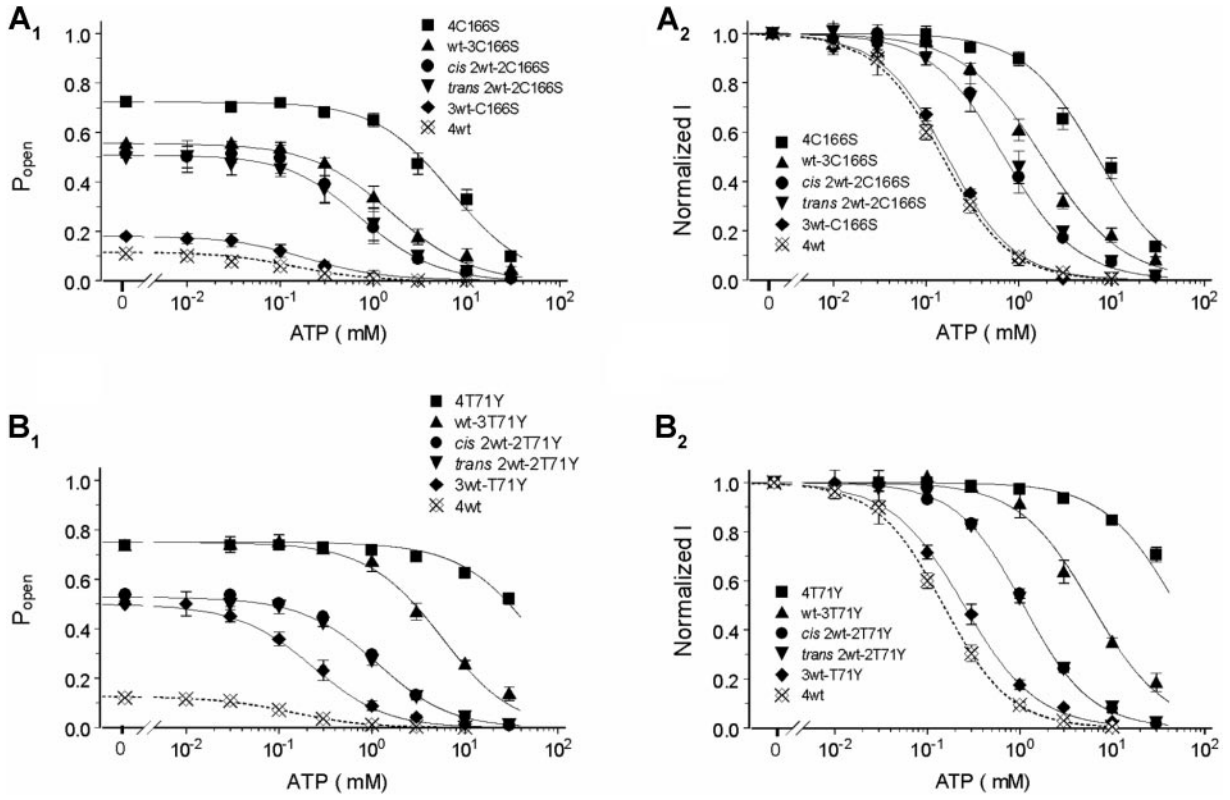

Fig. 5. The ATP sensitivity of tetramers with disruptions of channel gating. A_1 and A_2, the ATP-current relationship of the C166S tetramers. A_1, the dose-response relationship of these tetramers is fitted with eq. 5 according to basal P_{open} value of each C166S tetramer. The maximum inhibition reached 100% in these tetramers. Their basal P_{open} and IC_{50} values decrease with the addition of wt subunits. With three wt subunits, the ATP sensitivity of the 3wt-C166S is almost the same as the 4wt channel. The *cis* and *trans* 2wt-2C166S behaved just the same. A_2, the data were also fitted with Hill equation, and almost the same IC_{50} levels were obtained (Table 1). B_1 and B_2, similar results were obtained in tetrameric T71Y constructs with the same data analysis.

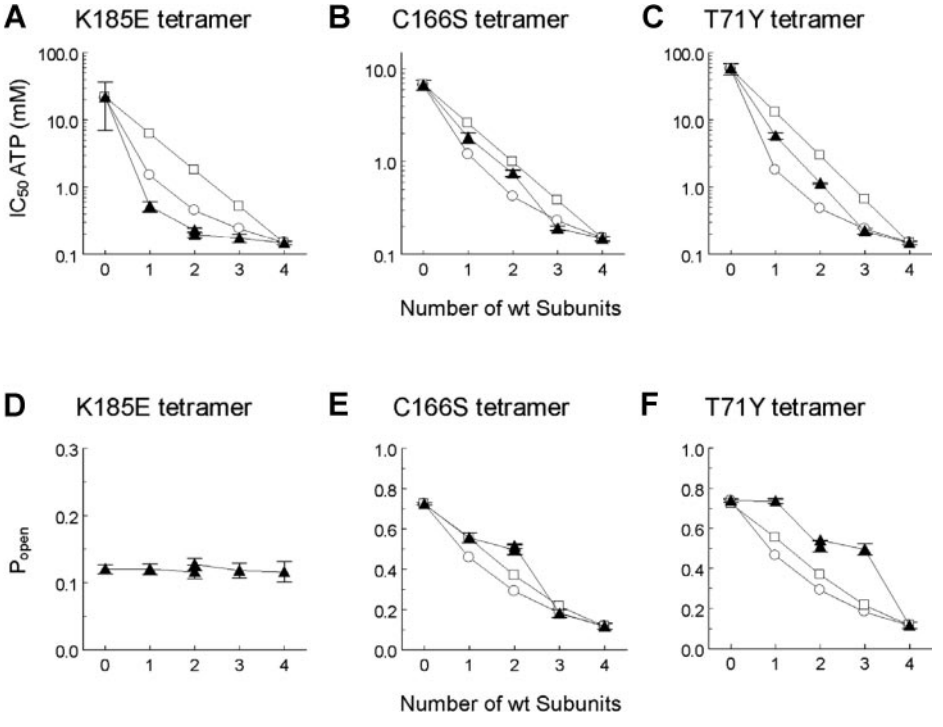

Fig. 6. Subunit cooperativity and coordination of the Kir6.2 channel. A–C, IC_{50} plots versus number of wt subunits. □, data predictions based on the MWC model; ○, data predictions based on the HH model. A, the IC_{50} plot of tetrameric K185E constructs (▲) is far from the MWC prediction and even runs below the HH prediction. B and C, unlike the K185E constructs, the plots of the C166S and T71Y tetramers are in between the predictions by the MWC and HH models. D–F, changes of basal P_{open} values with number of wt subunits. D, the basal P_{open} levels remain unchanged in all K185E mutations. E and F, the P_{open} plots of C166S and T71Y tetramers are both higher than the MWC prediction. Although each wt subunit decreases the basal P_{open} value, the greatest changes come with the first and third wt subunits in C166S tetramers and the second and fourth ones in T71Y tetramers.

completely blocked in the K185E-T71Y and K185E-C166S concatenated dimers; if the coupling were only mediated by two adjacent subunits (i.e., intersubunit coupling), it would be disabled in the wt-K185E/T71Y and wt-K185E/C166S constructs. The ATP sensitivity of these constructs was studied with the data fitted with operational model.

All of these constructs showed similar basal P_{open} values (range from 0.538 to 0.581, $P > 0.05$). The ATP sensitivity of the K185E-C166S and K185E-T71Y was well retained (both were fitted with the equation with IC_{50} = 1.20 mM, h = 1.0, τ = 0.42, and E_{max} = 48.2~49.4%) (Fig. 7, A and D, and Table 1), suggesting the existence of the intersubunit coupling.

The wt-K185E/T71Y responded to ATP exactly the same as the K185E-T71Y and K185E-C166S (Fig. 7, B and D, and Table 1). Higher ATP sensitivity was observed in the wt-K185E/C166S channel. Although the baseline P_{open} value was not much different from that of the wt-K185E/T71Y, the maximum inhibition (72.2%) was much greater (Fig. 7, C and D, and Table 1). Its ligand binding affinity was similar to all other dimers (K_A = 1.4~1.7), and its IC_{50} value (0.85 mM) shifted to the left without evident change in the h value. These results suggest that intrasubunit coupling also exists, and the intrasubunit coupling in the C terminus seems to contribute more to the channel gating than the intersubunit coupling.

To see whether the intrasubunit coupling in a single functional subunit is sufficient for the ATP-dependent gating, we constructed a tetramer by blocking all intra- and intersubunit couplings in three of the subunits using the wt-3C166S/K185E. Our test showed that there was no significant inhibition of this construct by intracellular ATP up to 30 mM (Fig. 7D), indicating that without intersubunit coupling, a single functional subunit is insufficient for the ATP-dependent gating.

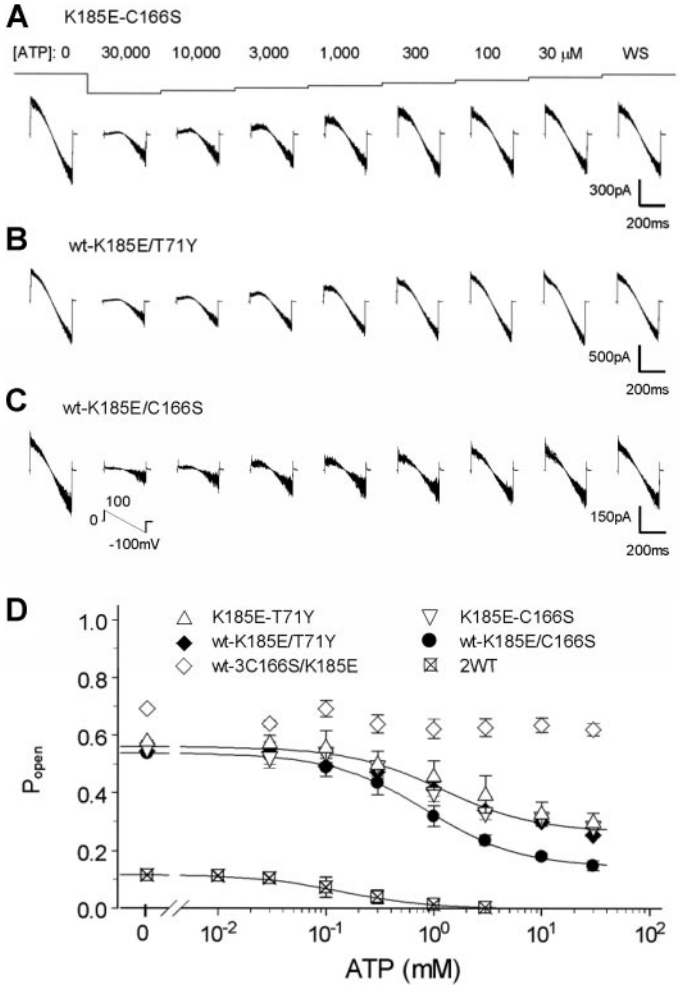

Fig. 7. The ATP sensitivity of dimers with disruptions of both ATP binding and channel gating. A, with the intrasubunit coupling mechanism being blocked in K185E-C166S channel, the currents were still sensitive to ATP, but the maximum inhibitory effect was only 50.6% with 30 mM ATP. B, the response was the same in the wt-K185E/T71Y dimer that only allow the intrasubunit coupling in alternative subunits. C, the similar intrasubunit coupling in the dimeric wt-K185E/C166S channels gave rise to a higher ATP sensitivity, and 72.2% maximum inhibition was reached. D, the ATP-current relationship curves of these dimers are fitted with operational model. All dimers have higher baseline channel activity than the 2wt channel. The dimeric K185E-C166S, K185E-T71Y and wt-K185E/T71Y show the same P_{open}, ATP sensitivity, and maximum inhibitory effect, so that their ATP-current relationships are fitted with a single equation. Greater ATP sensitivity and maximum inhibition are seen in the wt-K185E/C166S dimer. With only one functional subunit, the wt-3C166S/3K185E channel lost almost totally its ATP sensitivity.

Discussion

By selective disruption of ATP-binding or channel gating in a given number of subunits, our studies have revealed a number of events in ligand-dependent channel gating, suggesting that the concatemerization combined with the data analysis using the operational model is a powerful approach in understanding of the ligand-dependent channel gating.

ATP Binding Versus Channel Gating. The conformational changes produced by ligand binding may in turn affect the ligand binding affinity (Colquhoun, 1998), which was also shown previously in studies of the K_{ATP} channels (Tucker et al., 1998; Tsuboi et al., 2004). Therefore, the effects of ligand binding and channel gating are often entangled together, making the differentiation of binding from gating rather difficult. This problem is not limited to functional studies, because the conformational changes are known to affect results of binding assays as well (Colquhoun, 1998; Tsuboi et al., 2004). Differentiation of the binding from gating sites may be possible if 1) the protein X-ray crystallographic structure is resolved in presence of the ligand; 2) the binding affinity remains constant and is unaffected by subsequent conformational changes produced by ligand binding; or 3) there are special residues and protein domains that affect channel gating by one specific ligand but not another. The K_{ATP} channel seems to satisfy the latter criterion. Intense studies of the channel over the past decade have revealed several sites critical for ATP binding and channel gating.

The K185E-concatenated tetramers are special among all constructs. In addition to the graded loss of the ATP sensitivity with more disrupted subunits, we saw substantial residual channel activity that was not inhibited by ATP of up to 30 mM. The reduction in E_{max} value thus is consistent with previous findings in the CNG and HCN channels, indicating that ligand binding is disrupted (Liu et al., 1998; Paoletti et al., 1999; Young et al., 2001; Ulens and Siegelbaum, 2003; Young and Krougliak, 2004). The ATP-current relationship is very well expressed with the operational model. Basal P_{open} of K185E tetramers was not altered, whereas the maximum inhibition, efficacy, and IC_{50} were all reduced with stepwise subunit disruption. The predicated IC_{50} values for all K185E

constructs are almost identical with those measured with the Hill equation. Therefore, the model provides another level of understanding of the change in ATP sensitivity by taking into consideration the transient events in ligand binding and the following conformational changes.

Previous homology modeling has suggested that ATP interacts with several alkaline residues, including Arg50, Lys185, and Arg201 (Antcliff et al., 2005). Because they all contribute to ATP binding, mild mutation of an individual residue may not be sufficient to prevent ATP from interaction with the channel protein. At residue 185, for instance, mutation to a negatively charged but not a nonpolar residue causes almost complete loss of ATP sensitivity (Reimann et al., 1999). Therefore, we chose the K185E for our studies. Although the K185E was constructed in Kir6.2ΔC36 and expressed without SUR, its effect on residual currents has been observed in K185E-Kir6.2 expressed with SUR1 (Supplemental Fig. S3).

Unlike the K185E constructs, the C166S- and T71Y-concatenated tetramers were fully inhibited by high concentrations of ATP. However, subunit disruptions with the C166S and T71Y mutations increase not only the IC_{50} but also the basal P_{open} values. Both changes have been observed previously in monomeric C166S and T71Y and were explained to be a result of the disruption of the gating mechanism for channel closures (Trapp et al., 1998; Cui et al., 2003). It is possible that the Cys166 and Thr71 in the wt channel were necessary for the conformational changes of channel closures, which perhaps determine the conformational stability of closed states. Disruption of these residues leads to unstable closed states and augments basal P_{open}. Consistent with this idea, the P_{open} changes of the C166S and T71Y constructs are nicely described with τ_C in the operational model. Then why do the K_C and IC_{50} values increase with the disruption of two sites that are apparently not involved in ATP binding? As described above, ATP binds to closed states. Subunit disruption with the C166S or T71Y mutations may thus change the equilibrium constant for the gating transition between the open state and the ATP-unbound closed states, reducing the time expenditure in the closed states. As a consequence, higher concentrations of ATP are needed to inhibit the channel activity. The reduction in ATP binding affinity with the C166S mutation has been indicated previously (Tsuboi et al., 2004). The operational model may help to further understand the molecular basis. As shown by the operational model, multiple steps of conformational changes occur after ligand binding (Colquhoun, 1998; Trzeciakowski, 1999a,b; Kenakin, 2004). These steps are arranged in series. The conformational change of a given step depends on not only its previous step but also to a certain degree its successor. It is likely that the subunit disruption with the C166S or T71Y mutation impairs the necessary conformational change in a gating or coupling step (Trapp et al., 1998; Cui et al., 2003). Without the necessary conformational change in the step, its prior events, including the ATP binding affinity, are thus affected. Therefore, K_C value is determined by the conformational change of its predecessor (i.e., K_A and τ_A), and the K_C value changes produced by C166S or T71Y subunit disruptions also affect the IC_{50} value of ATP.

Coordination, Cooperativity, and Minimum Requirement of Functional Subunits. Our subunit stoichiometry studies have also revealed interesting subunit cooperativity, coordination, and minimum requirement of functional subunits for ATP binding and channel gating. Previous studies of the ATP-dependent gating in Kir6.2 channel suggest that the tetrameric channel has one ATP binding site in each subunit, and sequential bindings of four ATP molecules stabilize corresponding subunit to closed states, leading to inhibition of the channel activity (Enkvetchakul et al., 2000). Results from the present study indicate that the binding of each subsequent ATP molecule is also affected by the previous binding. Subunit disruption with the K185E mutation greatly reduces the ATP binding affinity and efficacy. The IC_{50} value of ATP decreases with the addition of wt subunits. The greatest change occurs with the introduction of the first wt subunit in the wt-3K185E, whereas smaller effects are seen with additional ones. The relationship of IC_{50} value with the number of wt subunits suggests strong negative cooperativity when it is compared with the HH and MWC models. Similar analysis of the C166S and T71Y constructs reveals positive cooperativity for channel gating, which was supported by both IC_{50} and P_{open} plots against the number of wt subunits. The presence of both negative cooperativity for ATP binding and positive cooperativity for channel gating may explain several previous observations showing no or modest positive cooperativity because the K_{ATP} channels have h values slightly greater than 1, and the h values remain unchanged with mutations of several critical residues for the ATP-dependent channel gating (Trapp et al., 1998; Reimann et al., 1999; Enkvetchakul et al., 2000; Markworth et al., 2000). In the P_{open} plot against the number of wt subunits, the basal P_{open} showed similar pattern of changes with the addition of every other wt subunits, indicating that the four subunits of the channel act as dimer of dimers. The same observation has been reported with the CNG, HCN, and Kir1.1 channels (Liu et al., 1998; Ulens and Siegelbaum, 2003; Wang et al., 2005a). The P_{open} plot also showed that the 4C166S and 4T71Y channels have similar basal P_{open} values, and these values are almost the same in 2wt-2C166S and 2wt-2T71Y tetramers. This suggests that the channel gating through the N or C terminus makes the same contribution when dimers are formed. On the other hand, wt subunits in C166S tetramers decrease the basal P_{open} much more than those in T71Y tetramers when dimers were not formed, which indicate that the gating through C terminus makes more contribution than through N terminus without subunit dimerization. It is reasonable because the movement of C terminus closes the channel directly, whereas the N terminus closes the channel through its interaction with the C terminus.

The channel gating does not show preference for *cis* or *trans* configurations. However, the channel with two wt subunits at the *cis* positions has a better ATP binding affinity and greater inhibitory efficacy than the *trans* configuration, suggesting that the ATP binding site is likely to be made of intracellular domains from multiple subunits, which is consistent with modeling studies based on the KirBac1.1 and KcsA channels (Antcliff et al., 2005). Our results suggest that such an ATP binding site may consist of at least two different subunits with two adjacent subunits surpassing two diagonal ones. The coordination between two subunits also suggests functional dimers that may be formed in the ATP-dependent channel gating. Supporting this idea are also the basal P_{open} plots. The basal P_{open} changes repeat when every other func-

tional subunit is introduced. These are consistent with previous demonstrations of dimer of dimers in CNG, HCN, and Kir1.1 channels (Liu et al., 1998; Ulens and Siegelbaum, 2003; Wang et al., 2005a). With the subunit coordination and cooperativity, two functional subunits seem adequate to achieve more than 90% of the ATP sensitivity. Indeed, the ATP-dependent channel gating cannot be fulfilled by a single wt subunit (wt-3C166S/K185E) without intersubunit coupling, although a functional subunit renders the channel substantial ATP sensitivity with intact intra- and intersubunit couplings (see the wt-3K185E in Figs. 3 and 4). Therefore, the ATP-dependent Kir6.2 channel gating requires a minimum of two functional subunits.

Potential Coupling Mechanisms. Another finding from the present study is that the effect of ligand binding can be coupled to channel gating not only within the same subunit (intrasubunit coupling) but also between two adjacent subunits (intersubunit coupling). Our results show that by blocking the intrasubunit coupling, the K185E-T71Y and K185E-C166S channels still respond to intracellular ATP, suggesting that the binding-gating-coupling is mediated by intersubunit interaction or intersubunit coupling. The result is consistent with the crystal structure of KirBac1.1 channel, indicating that the N terminus of one subunit contacts the C terminus of an adjacent subunit (Supplemental Fig. S1) (Kuo et al., 2003). Indeed, the structural modeling study suggests that ATP binding pocket of Kir6.2 channel is composed of the N and C terminus from two adjacent subunits (Antcliff et al., 2005). The intersubunit coupling through either N or C termini seems to have the same effect, because both K185E-T71Y and K185E-C166S retained approximately half of the maximum effect with the same IC_{50} level. However, the functional intrasubunit coupling in the C terminus (wt-K185E/C166S) seems to have greater effects on maximum inhibition (72.2%) and IC_{50} value than the intrasubunit coupling in the N terminus (wt-K185E/T71Y), suggesting that a stronger amplification exits via the backbone structure than that via interaction between protein domains of the same and alternate subunits. This idea is also supported by the result that introducing the first or third wt subunit in the C166S tetramers contributes more to the ATP sensitivity than in the T71Y tetramers.

Model for ATP Binding and Channel Gating. Based on the extended ternary operational model for ligand receptor interaction, we have developed a model to describe our results (Scheme 2). The model has four arms, with each representing one functional subunit. In each subunit, the ATP-dependent channel gating is initiated with ATP (A) binding to its binding site (R), and the binding affinity is determined by K_A. Ligand binding to the channel forms a ligand-receptor complex (AR), a fraction of which (AR*) produces the first step of conformational change. The fraction is determined by τ_A. The conformational change needs to be coupled to the physical gate in the same subunit, in which another conformational change (GAR*) controlled by τ_C occurs, leading to channel closure (intrasubunit coupling). Because the binding-coupling-gating is carried out by a series of conformational changes, disruption of an intermediate step in the coupling pathways, such as C166S and T71Y mutations, seems to compromise the coupling efficiency and require a greater conformational change in the step, which may not be fulfilled by the first step of conformational change with normal concentrations of ligand. The correct conformational change of the intermediate step is necessary for the successive step of conformational change and can in turn affect the consequence of the conformational change in a prior step. Thus, the τ_C not only determines the coupling efficiency but also controls the potency (i.e., IC_{50}). Four subunits in the channel do not act independently in the ligand gating. Each of the ATP binding sites seems to consist of two adjacent subunits. The ATP binding on one site reduces the binding affinity of the successive ATP binding (negative cooperativity). Therefore, the K_A is affected by the ATP binding on its adjacent subunits. Likewise, the conformational change in one subunit can be coupled to an adjacent subunit through intersubunit interaction or coupling, which is controlled by τ_C' for the coupling efficiency. Transition of each ligand-bound subunit between open and closed states facilitated the gating transition of successive subunits (positive cooperativity). Through subunit interaction, four subunits of the channel act as dimer of dimers. Because the K_C value is a function of the K_A and τ_A value with a relationship to be determined, and because the τ_C value affects the consequence of the first conformational change, the IC_{50} value of a channel therefore is determined by K_A, τ_A, and τ_C. With intact coupling mechanism (assuming the coupling efficiency is 100%), the IC_{50} value of K185E-concatenated tetramers is determined by the K_A and τ_A. With disruptions in the coupling pathways, channel gating requires greater τ_C, leading to an increase in the IC_{50}. The bottom level of the model refers to the spontaneous channel activation.

Our studies with the operational model described a number of events in the ATP-dependent channel gating. Although these events manifest themselves in different forms of concatemers with selective disruption of the ATP binding or channel gating, there is no doubt for their existence in the wt channels. Therefore, the operational model should also be useful in understanding intermediate events in ligand-dependent channel gating of wt channels by different ligands. Despite this, we emphasize that by introducing the operational model, we have no intension to replace several conventional kinetic models in ion channels studies. Indeed, the operational model involves more variables in data fitting and requires more sophisticated computation than the conven-

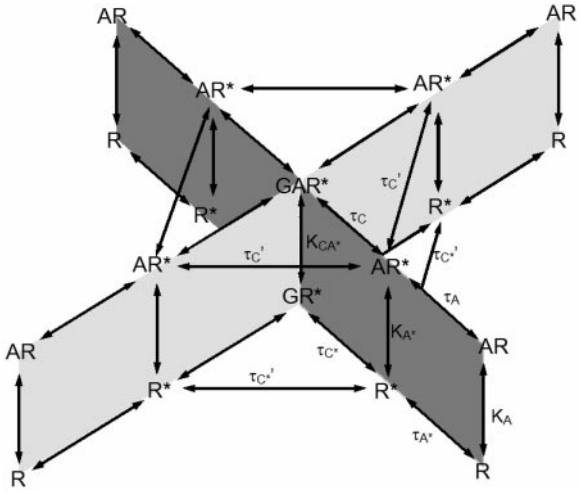

Scheme 2. Schematic model of the ATP-dependent Kir6.2 channel gating. See text for details.

tional kinetic models. Therefore, the conventional kinetic models may be more applicable in the description of channel gating when multiple intermediate states are not considered.

One of the questions remaining open is how the SUR subunit contributes to the channel gating. The SUR subunit augments the ATP sensitivity of the channel and may affect several intermediate events in channel gating. Clearly, further studies are needed to reveal the Kir6.2 channel gating by including the SUR subunit.

Acknowledgments

Special thanks to Dr. S. Seino at Kobe University in Japan for the gift of Kir6.2 cDNA.

References

Antcliff JF, Haider S, Proks P, Sansom MS, and Ashcroft FM (2005) Functional analysis of a structural model of the ATP-binding site of the K_{ATP} channel Kir6.2 subunit. *EMBO (Eur Mol Biol Organ) J* **24:**229–239.

Ashcroft FM and Gribble FM (1998) Correlating structure and function in ATP-sensitive K^+ channels. *Trends Neurosci* **21:**288–294.

Baukrowitz T, Schulte U, Oliver D, Herlitze S, Krauter T, Tucker SJ, Ruppersberg JP, and Fakler B (1998) PIP2 and PIP as determinants for ATP inhibition of K_{ATP} channels. *Science (Wash DC)* **282:**1141–1144.

Black JW and Leff P (1983) Operational models of pharmacological agonism. *Proc R Soc Lond B Biol Sci* **220:**141–162.

Colquhoun D (1998) Binding, gating, affinity and efficacy: the interpretation of structure-activity relationships for agonists and of the effects of mutating receptors. *Br J Pharmacol* **125:**924–947.

Cui N, Wu J, Xu H, Wang R, Rojas A, Piao H, Mao J, Abdulkadir L, Li L, and Jiang C (2003) A threonine residue (Thr71) at the intracellular end of the M1 helix plays a critical role in the gating of Kir6.2 channels by intracellular ATP and protons. *J Membr Biol* **192:**111–122.

Del Castillo J and Katz B (1957) Interaction at end-plate receptors between different choline derivatives. *Proc R Soc Lond B Biol Sci* **146:**369–381.

Enkvetchakul D, Loussouarn G, Makhina E, Shyng SL, and Nichols CG (2000) The kinetic and physical basis of K_{ATP} channel gating: toward a unified molecular understanding. *Biophys J* **78:**2334–2348.

Flynn GE and Zagotta WN (2001) Conformational changes in S6 coupled to the opening of cyclic nucleotide-gated channels. *Neuron* **30:**689–698.

Hodgkin AL and Huxley AF (1952) A quantitative description of membrane current and its application to conduction and excitation in nerve. *J Physiol* **117:**500–544.

Jiang Y, Lee A, Chen J, Cadene M, Chait BT, and MacKinnon R (2002) Crystal structure and mechanism of a calcium-gated potassium channel. *Nature (Lond)* **417:**515–522.

Jin T, Peng L, Mirshahi T, Rohacs T, Chan W, Sanchez KR, and Logothetis DE (2002) The beta-gamma subunits of G proteins gate a K^+ channel by pivoted bending of a transmembrane segment. *Mol Cell* **10:**469–481.

John SA, Weiss JN, and Ribalet B (2005) ATP sensitivity of ATP-sensitive K^+ channels: role of the gamma phosphate group of ATP and the R50 residue of mouse Kir6.2. *J Physiol (London)* **568:**931–940.

Kenakin T (2004) Principles: receptor theory in pharmacology. *Trends Pharmacol Sci* **25:**186–192.

Kuo A, Gulbis JM, Antcliff F, Rahman JT, Lowe ED, Zimmer J, Cuthbertson J, Ashcroft FM, Ezaki T, and Doyle DA (2003) Crystal structure of the potassium channel KirBac1.1 in the closed state. *Science (Wash DC)* **300:**1922–1926.

Liu DT, Tibbs GR, Paoletti P, and Siegelbaum SA (1998) Constraining ligand-binding site stoichiometry suggests that a cyclic nucleotide-gated channel is composed of two functional dimers. *Neuron* **21:**235–248.

Markworth E, Schwanstecher C, and Schwanstecher M (2000) ATP^{4-} mediates closure of pancreatic beta-cell ATP-sensitive potassium channels by interaction with 1 of 4 identical sites. *Diabetes* **49:**1413–1418.

Monod J, Wyman J, and Changeux JP (1965) On the nature of allosteric transitions: a plausible model. *J Mol Biol* **12:**88–118.

Noma A (1983) ATP-regulated K^+ channels in cardiac muscle. *Nature (Lond)* **305:**147–148.

Paoletti P, Young EC, and Siegelbaum SA (1999) C-Linker of cyclic nucleotide-gated channels controls coupling of ligand binding to channel gating. *J Gen Physiol* **113:**17–34.

Perozo E, Cortes DM, and Cuello LG (1999) Structural rearrangements underlying K^+-channel activation gating. *Science (Wash DC)* **285:**73–78.

Phillips LR, Enkvetchakul D, and Nichols CG (2003) Gating dependence of inner pore access in inward rectifier K^+ channels. *Neuron* **37:**953–962.

Piao H, Cui N, Xu H, Mao J, Rojas A, Wang R, Abdulkadir L, Li L, Wu J, and Jiang C (2001) Requirement of multiple protein domains and residues for gating K_{ATP} channels by intracellular pH. *J Biol Chem* **276:**36673–36680.

Reimann F, Ryder TJ, Tucker SJ, and Ashcroft FM (1999) The role of lysine 185 in the kir6.2 subunit of the ATP-sensitive channel in channel inhibition by ATP. *J Physiol* **520:**661–669.

Ribalet B, John SA, and Weiss JN (2003) Molecular basis for Kir6.2 channel inhibition by adenine nucleotides. *Biophys J* **84:**266–276.

Seino S (1999) ATP-sensitive potassium channels: a model of heteromultimeric potassium channel/receptor assembly. *Annu Rev Physiol* **61:**337–362.

Shyng SL and Nichols CG (1998) Membrane phospholipid control of nucleotide sensitivity of K_{ATP} channels. *Science (Wash DC)* **282:**1138–1141.

Trapp S, Haider S, Jones P, Sansom MS, and Ashcroft FM (2003) Identification of residues contributing to the ATP binding site of Kir6.2. *EMBO (Eur Mol Biol Organ) J* **22:**2903–2912.

Trapp S, Proks P, Tucker SJ, and Ashcroft FM (1998) Molecular analysis of ATP-sensitive K channel gating and implications for channel inhibition by ATP. *J Gen Physiol* **112:**333–349.

Trzeciakowski JP (1999a) Stimulus amplification, efficacy, and the operational model. Part I—binary complex occupancy mechanisms. *J Theor Biol* **198:**329–346.

Trzeciakowski JP (1999b) Stimulus amplification, efficacy, and the operational model. Part II—ternary complex occupancy mechanisms. *J Theor Biol* **198:**347–374.

Tsuboi T, Lippiat JD, Ashcroft FM, and Rutter GA (2004) ATP-dependent interaction of the cytosolic domains of the inwardly rectifying K^+ channel Kir6.2 revealed by fluorescence resonance energy transfer. *Proc Natl Acad Sci USA* **101:**76–81.

Tucker SJ, Gribble FM, Proks P, Trapp S, Ryder TJ, Haug T, Reimann F, and Ashcroft FM (1998) Molecular determinants of K_{ATP} channel inhibition by ATP. *EMBO (Eur Mol Biol Organ) J* **17:**3290–3296.

Tucker SJ, Gribble FM, Zhao C, Trapp S, and Ashcroft FM (1997) Truncation of Kir6.2 produces ATP-sensitive K^+ channels in the absence of the sulphonylurea receptor. *Nature (Lond)* **387:**179–183.

Ulens C and Siegelbaum SA (2003) Regulation of hyperpolarization-activated HCN channels by cAMP through a gating switch in binding domain symmetry. *Neuron* **40:**959–970.

Wang R, Su J, Wang X, Piao H, Zhang X, Adams CY, Cui N, and Jiang C (2005a) Subunit stoichiometry of the Kir1.1 channel in proton-dependent gating. *J Biol Chem* **280:**13433–13441.

Wang R, Su J, Zhang X, Shi Y, and Jiang C (2005b) Kir6.2 channel gating by intracellular protons: subunit stoichiometry for ligand binding and channel gating. *Soc Neurosci Abstr* **31:**609.1.

Wu J, Cui N, Piao H, Wang Y, Xu H, Mao J, and Jiang C (2002) Allosteric modulation of the mouse Kir6.2 channel by intracellular H^+ and ATP. *J Physiol* **543:**495–504.

Wu J, Piao H, Rojas A, Wang R, Wang Y, Cui N, Shi Y, Chen F, and Jiang C (2004) Critical protein domains and amino acid residues for gating the KIR6.2 channel by intracellular ATP. *J Cell Physiol* **198:**73–81.

Xu H, Cui N, Yang Z, Wu J, Giwa LR, Abdulkadir L, Sharma P, and Jiang C (2001) Direct activation of cloned K_{ATP} channels by intracellular acidosis. *J Biol Chem* **276:**12898–12902.

Young EC and Krougliak N (2004) Distinct structural determinants of efficacy and sensitivity in the ligand-binding domain of cyclic nucleotide-gated channels. *J Biol Chem* **279:**3553–3562.

Young EC, Sciubba DM, and Siegelbaum SA (2001) Efficient coupling of ligand binding to channel opening by the binding domain of a modulatory (beta) subunit of the olfactory cyclic nucleotide-gated channel. *J Gen Physiol* **118:**523–546.

Address correspondence to: Dr. Chun Jiang, Department of Biology, Georgia State University, 24 Peachtree Center Avenue, Atlanta, GA 30302-4010. E-mail: cjiang@gsu.edu